Migration behaviour of selenium implanted into polycrystalline 3C-SiC

ZAY Abdalla[1,*], MYA Ismail[1], EG Njoroge[1], TT Hlatshwayo[1], E Wendler[2], JB Malherbe[1]

[1]*Department of Physics, University of Pretoria, Pretoria 0002, South Africa*

[2]*Institut für Festkörperphysik, Friedrich-Schiller Universität Jena, 07743 Jena, Germany*

ABSTRACT

The migration behaviour of selenium (Se) implanted into polycrystalline SiC was investigated using Rutherford backscattering spectrometry (RBS), scanning electron microscopy (SEM) and Raman spectroscopy. Se ions of 200 keV were implanted into polycrystalline SiC samples to a fluence of 1×10^{16} cm^{-2} at room temperature. The implanted samples were isochronal annealed in vacuum at two different regimes. Initially, the samples were annealed from 1000 to 1500 ºC in steps of 100 ºC for 10 hours. Another set, at 1300 ºC, 1350 ºC and 1450 ºC for 20 hours. Implantation of Se at room temperature amorphized the near-surface region of the SiC substrate. Annealing at 1000ºC already resulted in the recrystallization of the amorphous SiC. The SEM images showed that the polishing marks became less visible after implantation due to the sputtering and swelling effects. These crystallites became larger and more visible with increase in annealing temperature. No diffusion was observed for annealing up to 1200°C. Slight peak broadening indicating diffusion was observed after annealing at 1300°C. This broadening increased with increase in annealing temperature. In the second set of annealing, the diffusion coefficients at 1300 and 1350 °C were estimated to be 6.3×10^{-21} and 2.0×10^{-20} m^2 s^{-1}, respectively.

Keywords: Diffusion, Polycrystalline SiC, Raman spectroscopy, RBS, SEM

1. INTRODUCTION

Silicon carbide (SiC) is considered as one of the few lightweight covalently bonded ceramics with interesting properties, such as a low thermal expansion coefficient and high thermal conductivity, mechanical strength and hardness [1]. The outstanding properties of SiC, make it suitable for applications in the petrochemical and specifically, for the purpose of this work, in the nuclear industries [2]. The safety of modern nuclear reactors depends on the retainment of all the radioactive fission products that may leak into the environment during its operation [3]. In the Pebble Bed Modular Reactor (PBMR), which is one of Very High Temperature Reactors (VHTR), the containment of fission products (FP) within Tristructural-isotropic (TRISO) fuel particles is critical for the successful and safe operation of the reactor. The SiC layer is a very important regarding these particles because it has a number of very crucial functions, such as structural support and acting as the main diffusion barrier for fission products [4][5].

Selenium (Se) is a non-metallic element with atomic number 34. It has many radioactive isotopes such as ^{72}Se, ^{75}Se, ^{79}Se, ^{80}Se and ^{82}Se. ^{79}Se is a component of spent nuclear fuel, and is found in high-level radioactive wastes resulting from processing spent fuel associated with the operation of nuclear reactors and fuel reprocessing plants. Although the low percentage yield of selenium formed by uranium fission, as in a nuclear reactor, the risk comes from leaking this amount into the environment for a long term. The health hazards of ^{79}Se come from the beta particles emitted during its radioactive decay, and the main concern is associated with the increased likelihood of inducing cancer [6]. ^{80}Se is one of the stable isotopes, the most prevalent, comprising about half of natural selenium [6]. It is both naturally occurring and produced by fission [7].

The extremely low diffusivities for impurities in SiC is one of the reasons SiC is used as the fission product barrier in TRISO fuel [8]. The migration behaviour of fission products such as strontium, iodine, cesium and silver in SiC at temperatures above 1000°C have been studied extensively [9]. There is no reported information on the migration behaviour of selenium in SiC.

In this study, we investigate the migration behaviour of ^{80}Se implanted into polycrystalline 3C-SiC at room temperature to a fluence of 1×10^{16} cm^{-2} at temperatures above 900°C.

2. EXPERIMENTAL PROCEDURE

Polycrystalline SiC wafers from Valley Design Corporation were used in this investigation. These wafers were composed of mainly 3C-SiC with some traces of 6H-SiC [10]. Se ions with an energy of 200 keV were implanted into the SiC wafers to a fluence of 1×10^{16} cm^{-2} at room temperature. The implantation was performed at the Friedrich-Schiller-University Jena, Germany. Some of the implanted samples were isochronal annealed in vacuum using a computer controlled Webb 77 graphite furnace at temperatures ranging from 1000 to 1500°C in steps of 100°C for 10 hours. Se profiles of the as-implanted and annealed samples were monitored using Rutherford backscattering spectrometry (RBS), implementing the Van de Graaff accelerator at the University of Pretoria. RBS was performed at room temperature using He^+ particles at 1.6 MeV. The beam current was approximately 15 nA and 8 μC charge was collected per measurement. The RBS spectra were converted to depth in nm using the energy loss data and density of pristine SiC (3.21 gcm^{-3}). The depth profiles were fitted to a Gaussian function to extract the projected ranges (Rp) and stragglings (ΔRp) for each sample. They were also fitted to the solution of the Fick diffusion equation for a Gaussian as-implanted profile to extract the diffusion coefficients [11]. The topographies of the surfaces before and after annealing were

investigated by a Zeiss Ultra 55 field emission gun scanning electron microscopy (FEG-SEM) with an in-lens detector. An accelerating voltage of 2 kV was used. The microstructural changes in SiC due to the implantation and annealing were monitored by using a Jobin Yvon, Horiba(C) TX64000 triple Raman spectrometer. The investigations were performed in the visible region with a 514.5 nm of Ar/Kr laser lines as exciting radiation. The spot of ~2μm^2 was used to focus the laser beam and collected by a 50X objective.

3. RESULTS AND DISCUSSION

3. 1 RBS

In Fig. 1, the measured as-implanted Se depth profile, the simulated Se profile and simulated damage in displacement per atom (dpa) are shown. The simulations were performed using SRIM 2013 [12], assuming a displacement energy (E_d) of 20 eV and 35 eV for C and Si respectively [10]. The radiation damage from SRIM 2013 was converted into displacements per atom (dpa) using equation 1[13]:

$$dpa = \frac{(\nu_{ca}/ion\text{Å})\times 10^{8} \times \varphi\,(ions\ cm^{-2})}{\rho_{SiC}\,(atoms\ \ cm^{-3})} \tag{1}$$

where, $(\nu_{ca}/ion\text{Å})$ is the vacancy per ion from SRIM 2012, φ is the ion fluence (1×10^{16} cm^{-2}), ρ_{SiC} is the density of silicon carbide (3.21g cm^{-3}).

The experimental projected range (Rp) of 87.7 nm was slightly lower than the theoretical value of 89.6 nm. The value obtained is within the experimental error of the RBS measurements about 5% and the uncertainties of the SRIM simulations. The experimental straggling (ΔRp) value is about 11% larger than that obtained by theoretical simulation viz. 29.9 and 26.5 nm, respectively. This discrepancy in the ΔR_P may be attributed to the fact that re-distribution of Se is already taking place during the implantation process. The implanted selenium profile is almost a

Gaussian distribution with the kurtosis (β = 2.9) and skewness (γ = 0.28). These values are very close to those of the true Gaussian distribution (β = 3) and (γ = 0). What is also evident in Fig. 1 is that the maximum damage of about 1.3 dpa is at about 70 nm below the surface as compared to the experimental Rp of 87.7 nm. If one assumes that 0.3 dpa amorphises SiC [14], it is quite clear that a 125 nm layer of SiC below the surface is amorphized. From these results it is quite clear that the majority of implanted Se is embedded in the amorphous SiC.

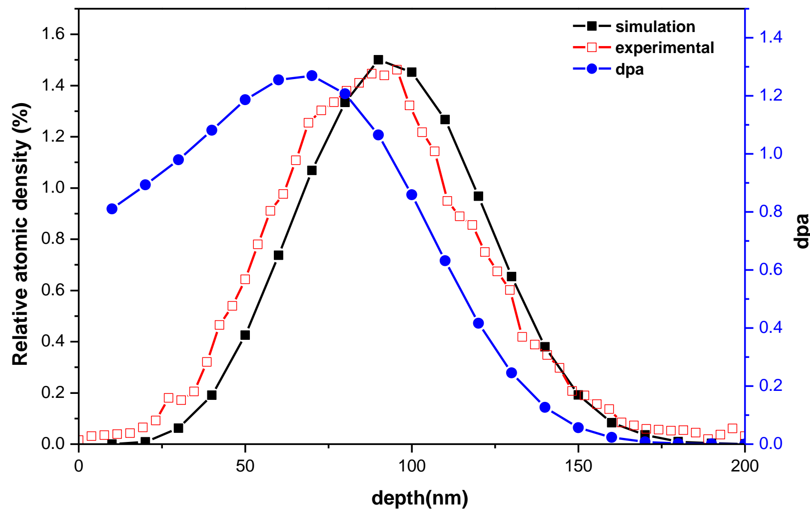

Fig. 1. The depth profile of Se implanted into SiC from RBS, SRIM 2012 simulated Se depth profile and damage in displacement per atom (dpa).

To investigate the migration behaviour of Se in polycrystalline SiC, the implanted samples were subjected to sequential isochronal annealing at temperatures ranging from 1000 to 1500 °C in steps of 100 °C for 10 hours. The Se depth profiles obtained from RBS before and after annealing are shown in Fig. 2. Neither a change in the implanted Se profile nor broadening was observed after annealing from 1000 up to 1200 °C. This observation indicated the lack of detectable diffusion after annealing

at these temperatures. A slight broadening of the implanted Se profile was observed after annealing at 1300 °C as can be seen in Figs. 2 and 3. However, both were within the experimental error of the depth scale of our RBS measurements. The broadening became more significant after annealing at 1400 °C and 1500°C. The broadening of the profile is an indication of diffusion of the Se implanted ions [11]. It is also clear that the annealing at 1300 °C and 1400 °C led to the removal of the SiC layer by thermal etching, which moved the selenium profile towards the surface, resulting in the loss of some of the implanted Se (see Fig. 3). The annealing at a temperature of 1500 °C led to the decomposition of silicon carbide, as is evident in the formation of the carbon layer on top of the carbon surface (see Fig. 4). What was also noticeable was a general decrease in the heights of the Se profiles. To quantify this, the total integrated counts of the RBS Se signal (counts) were taken. The results are shown in Fig. 3. There was also a very slight asymmetry near the surface (i.e. x = 0) in the Se profiles at 1400 °C and 1500 °C. There are two possible reasons for this, namely segregation towards the surface and evaporation into the vacuum of the Se atoms which diffused to the surface. The boiling point of Se is 685°C is significantly less than the annealing temperatures.

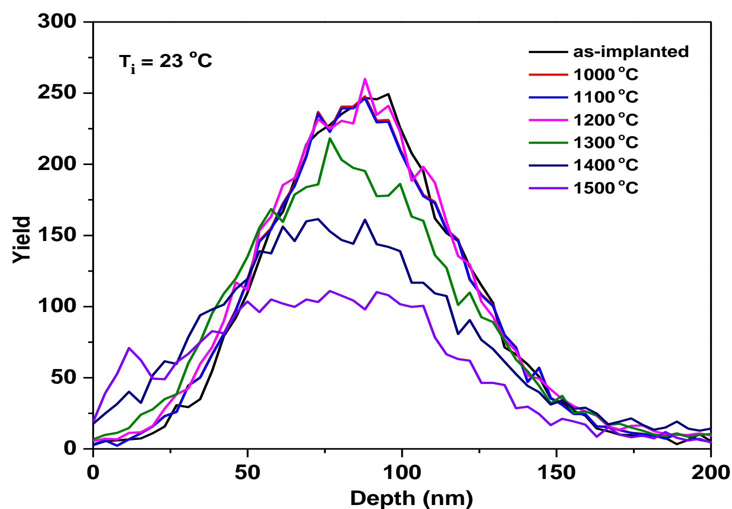

Fig.2. Depth profiles of selenium implanted in 3C–SiC at room temperature and after sequential isochronal annealing from 1000 to 1500 °C for 10 hours.

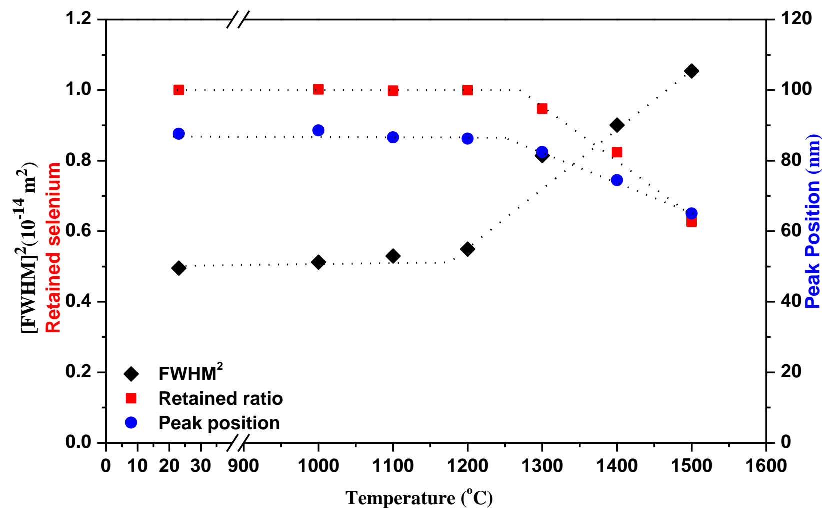

Fig. 3. The full width at half maximum, the peak position of implanted Se, and retained ratio (calculated as the ratio of the total integrated counts of Se after annealing to that of as-implanted) of the Se profile as a function of annealing temperature.

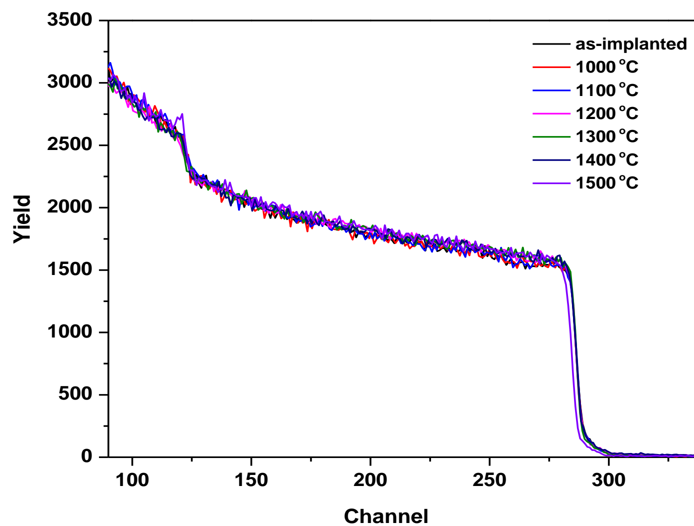

Fig.4. RBS spectra of selenium implanted in 3C–SiC at room temperature and after isochronal annealing from 1000 to 1500 °C for 10 hours.

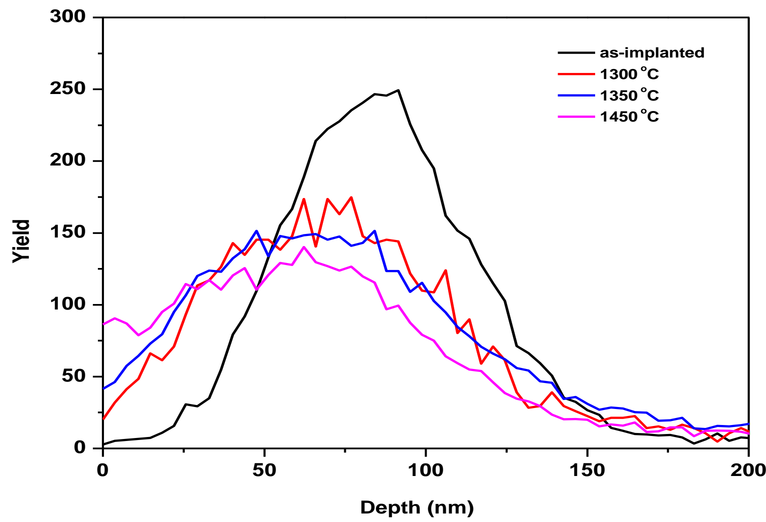

Fig.5. Depth profiles of selenium implanted in 3C–SiC at room temperature and after isochronal annealing at1300, 1350 and 1450 °C for 20 hours.

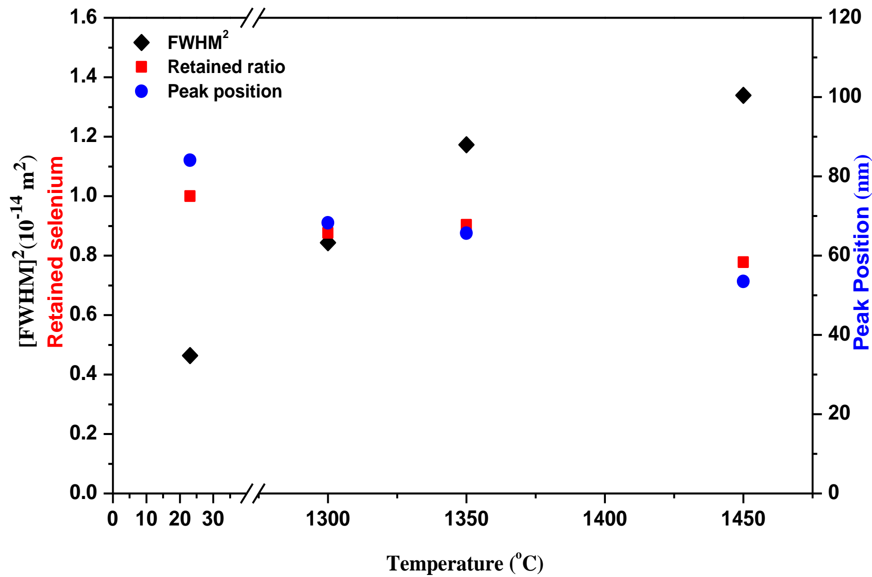

Fig. 6. The full width at half maximum, the peak position of implanted Se, and retained ratio (calculated as the ratio of the total integrated counts of Se after annealing to that of as-implanted) of the Se profile as a function of annealing temperature.

A new as-implanted sample was subjected to isochronal annealing at three different temperatures for 20 hours as shown in Fig. 5, and it was found that the profile broadens and shifts toward the surface (see Fig. 6). There was also a significant loss of implanted ions (see Fig. 6). To extract the diffusion coefficient of Se implanted into polycrystalline SiC, the Se depth profiles obtained from RBS were fitted to the solution of Fick's diffusion equation for Gaussian as-implanted profile and with a perfect sink at the surface (see Fig. 7) [11]. The diffusion coefficients of 6.3×10^{-21} and 2.0×10^{-20} m^2s^{-1} were extracted at 1300 and 1350 °C respectively. The diffusion coefficient at 1450 °C could not be determined because the Se profile deviated from the diffused profile derived in [11]. This deviation was cause a segregation towards the surface.

There have been no reports on Se diffusion in SiC. Hence the obtained diffusion coefficients were not compared with any other literature values.

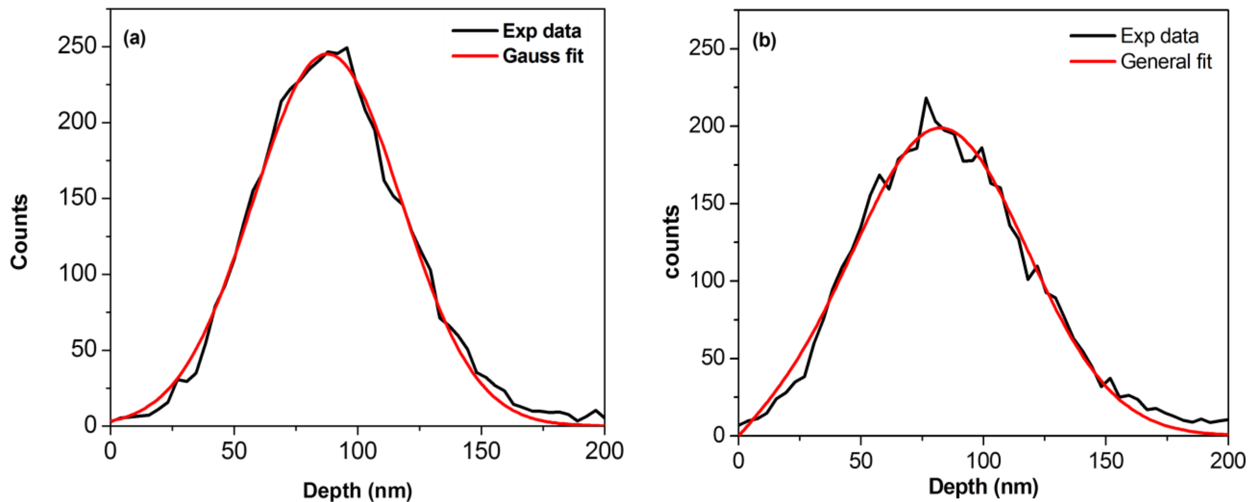

Fig. 7. Example of the fitting of the diffusion equation solution to the depth profiles of the sample (a) as-implanted, (b) annealed at 1300 ^oC for 10 h.

3. 2 SEM

The SEM images of as-implanted and annealed samples are shown in Fig. 8 A SEM image of a pristine sample after polishing is included for comparison. The surface of the pristine sample contains some polishing marks as can be seen in Fig. 8(a), while (b) shows that the polishing marks became less pronounced after implantation due to the sputtering of the SiC surface by the bombarding Se ions, and the swelling of the amorphous implanted layer [15]. After annealing at 1000 °C (Fig. 8(c)), the surface remained flat and featureless. The higher magnification insert shows evidence of recrystallization. After annealing at 1300°C (Fig. 8(d)), the crystals became more apparent and distinct than in the sample annealed at 1000 °C. Some cavities can also be seen. The higher magnification clearly shows that some large crystals are on top of the smaller crystals, with the latter forming a kind of a substrate. The variation in the height indicates an increasing surface roughness, which is more apparent in the low magnification image. The smaller crystals increased in size after annealing at 1400°C (Fig. 8(e). Consequently, the distinction between large and smaller crystals became less obvious with fewer but larger pores. The uniformity of distribution in crystal size is seen after annealing at 1500°C (Fig. 8(f). The pores became more prominent. These pores may explain the loss of significant amounts of the implanted Se ions at this temperature.

Fig. 9(a) shows that the annealing of an as-implanted sample at 1300 ºC for 20 hours led to the appearance of large crystals with a few pores. After annealing at higher temperatures (1350 and 1450 ºC), the crystals became more prominent (Fig. 9(b) and (c)). The 1450 ºC samples (Fig. 9(c)) had slightly more and longer dendritic crystals.

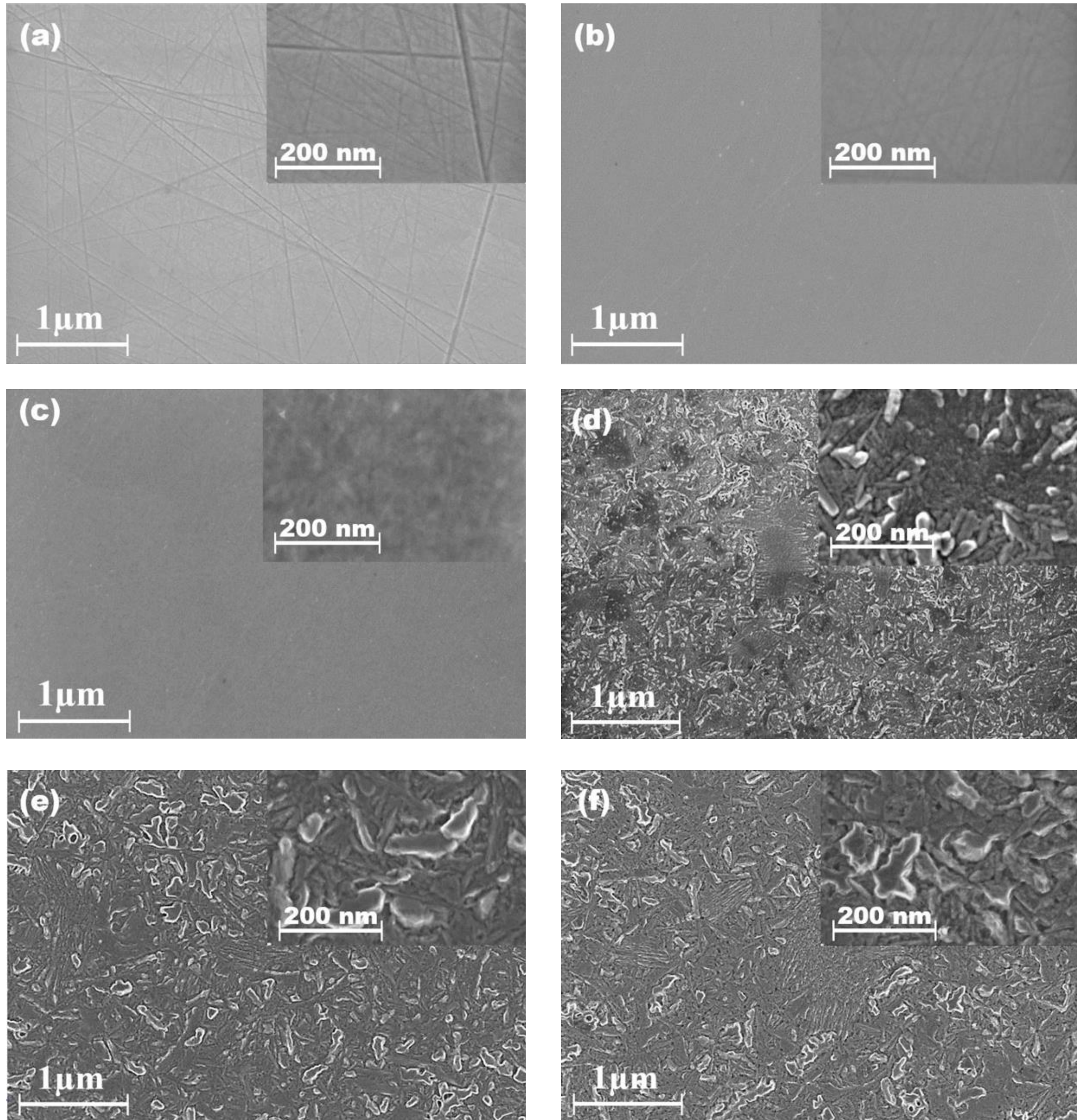

Fig. 8. Surface SEM micrographs of (a) Pristine poly-SiC; (b) after implantation with Se at RT; compared with surfaces after vacuum annealing at (c)1000 °C, (d) 1300 °C, (e) 1400 °C and (f) 1500°C for 10 hours.

.

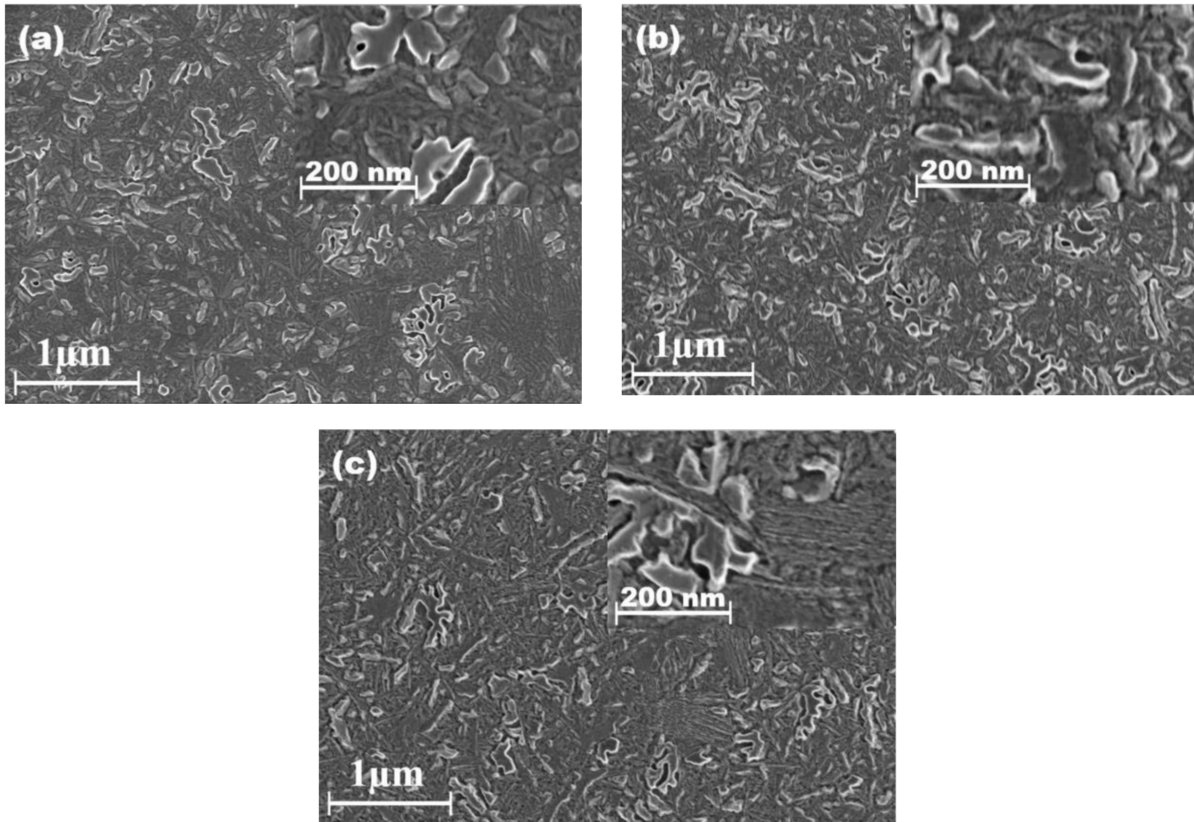

Fig. 9. Surface SEM micrographs of as-implanted SiC after vacuum annealing at (a) 1300 °C, (b) 1350 °C and (c) 1450 °C for 20 hours.

3. 3 Raman Results

Fig.10(a) and (b) show the Raman spectra of pristine sample, an as-implanted and an annealed sample from1000 to 1500°C in steps of 100°C for 10 h. The spectrum obtained from the pristine sample showed a number of Raman lines indicating silicon carbide, which include the transverse optical (TO) mode splitting into two peaks at 771 and 797 cm^{-1}, the longitudinal optical (LO) mode at 966.5 cm^{-1}, a TO overtone peak at 1520 cm^{-1} and another overtone at 1714 cm^{-1}. These values are very close to those reported in references [16][17][18].

From spectra of the as-implanted (see Fig. 10(a)), it is clear that the characteristic SiC Raman peaks (between 750 and 1000 cm^{-1}) disappeared and three broad Raman bands appeared around 519, 880 and 1424 cm^{-1}. These broad bands are caused by the vibrations of Si-Si, Si-C and C-C bonds, respectively [19]. This change in the spectrum indicates that the SiC layer is amorphized as a result of the implantation. After annealing at 1000°C, the main Raman peaks of silicon carbide were observed indicating the recovery of the crystal SiC structure.

The detection of defects can be monitored with the longitudinal optical (LO) Raman mode [20]. In this study, the characterization of the recovery process is based on the measurements of the shift and linewidth of the LO mode as a function of temperature. Annealing at 1000 °C resulted in the appearance of the LO peak at 962.2 cm^{-1}, which is 4.3 cm^{-1} lower than the one of the virgin sample as can be seen in Fig. 11 (a). This indicates the presence of the tensile stress in bonds between atoms as a result of a change in atomic distances [21] . After annealing at 1100 °C, the LO peak shifted by 2.6 cm^{-1} towards a higher wavenumber, suggesting less tensile stress. Further annealing shows that the LO peak shifted again toward lower wavenumbers, indicating higher tensile stress. Fig. 11 (a) also shows that the FWHM of LO mode obtained from the sample annealed at 1000 °C (12.4 cm^{-1}) is broader in comparison with the virgin sample (9.6 cm^{-1}). The broadness of the Raman band indicates the presence of defects and a poor crystallinity [22]. With increased annealing temperature, the FWHM decreased gradually and became 10.6 cm^{-1}, which is broader than the one observed in the virgin indicating that defects are still present.

From the Raman results of the sample implanted at room temperature and annealed for 20 h at temperatures of 1300 °C, 1350 °C and 1450 °C (not shown), the LO mode appeared at approximately 963 cm^{-1} after annealing at 1300 °C. It can be clearly observed to shift towards a lower wavenumber with increasing temperature to approximately 962.5cm^{-1} after annealing at 1350 °C and 1450 °C as shown in Fig.

11 (b), which implies the presence of tensile stress inside the sample. Fig. 11 (b) also shows that the FWHM decreased from 11.4 cm^{-1} after annealing at 1300 C to 11.3 cm^{-1} after annealing at 1350 C. After annealing at 1450 °C, the FWHM became 10.5 cm^{-1}, suggesting that the sample has approximately the same degree of crystallization as the one annealed at 1500 ° C for 10 h.

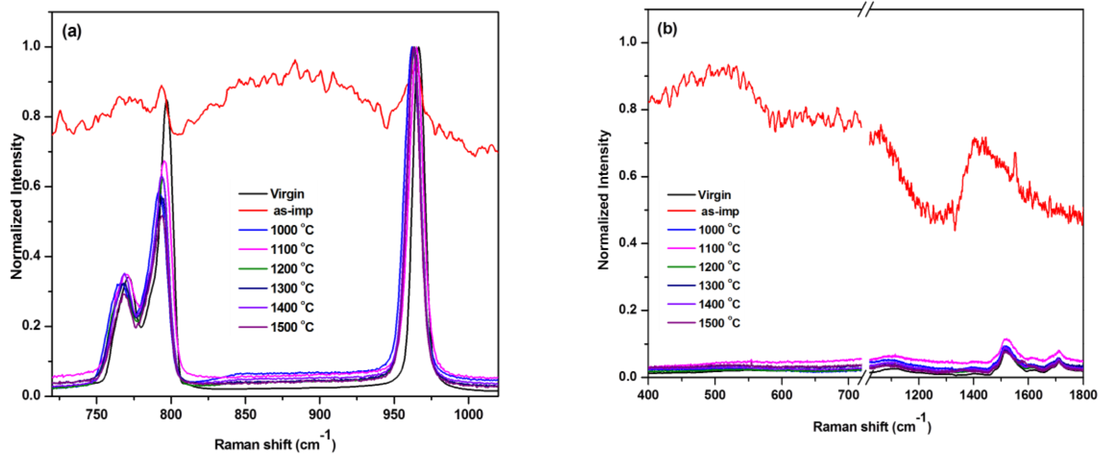

Fig. 10. (a) First order, (b) Second order Raman spectra of the pristine 3C-SiC after implantation and sequential isochronal annealing from 1000 to 1500 °C for 10 hrs.

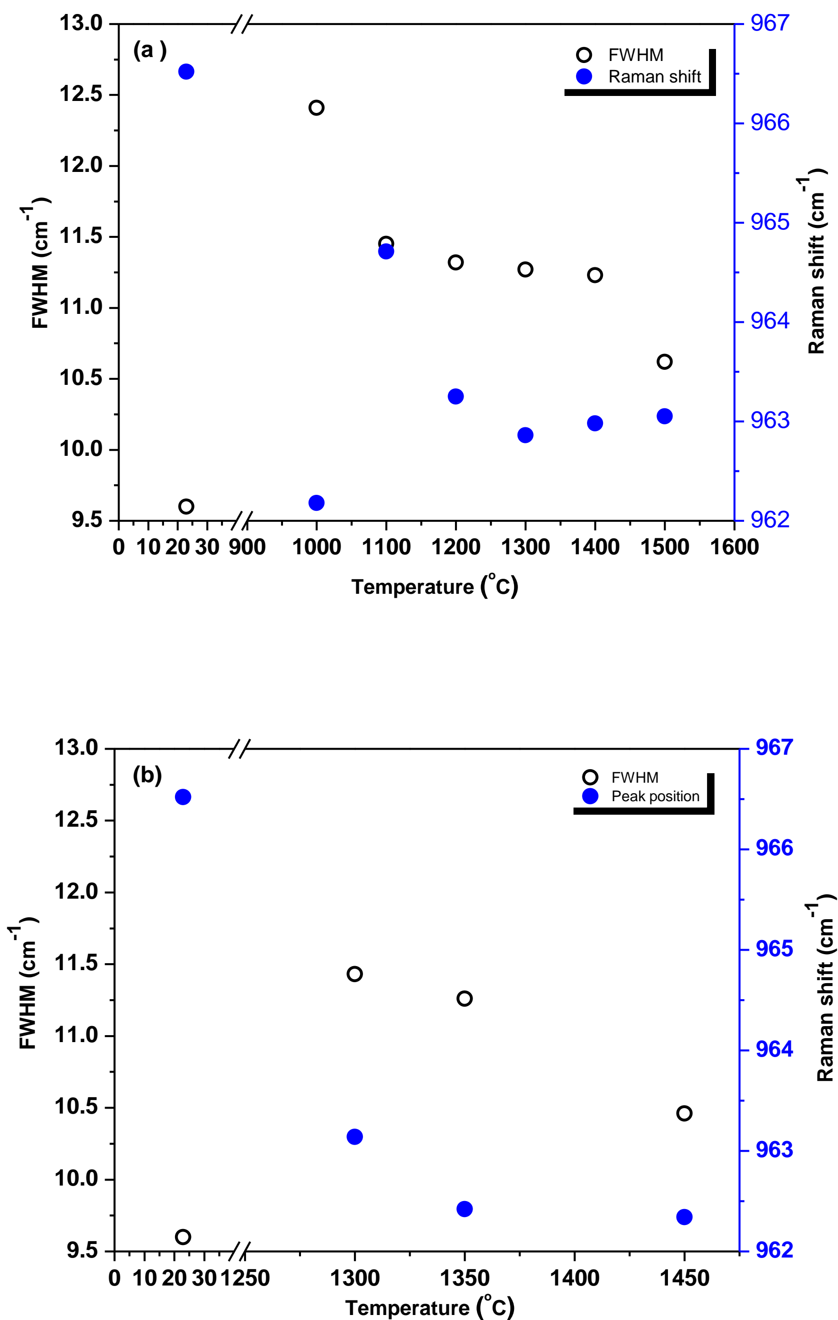

Fig. 11. The FWHM and Raman shift of the LO mode as function of temperature (a) after sequential isochronal annealing from 1000 to 1500 °C for 10 hrs, (b) after annealing at 1300 °C, 1350 °C and 1450 °C for 20 hrs.

4. CONCLUSION

In this study, the migration behaviour of Se in polycrystalline SiC was investigated in terms of diffusion and structural change. The RBS depth profiles showed that no diffusion occurred after annealing at temperatures from 1000 up to 1200°C. The thermal etching at higher temperatures caused the Se profile to shift toward the surface, where the Se ions evaporated. The shift was accompanied by loss of Se from the surface. Significant losses of about 40% and 20% were observed at 1500°C (10 h) and 1450°C (20 h), respectively. SEM results show that the implantation resulted in less visible polishing marks. It also showed that annealing has a significant effect on the crystals growth on the surface of SiC. The Raman results show that the SiC layer became amorphized after implantation, and recrystallization started after annealing at 1000 ºC, as well as the presence of tensile stress inside the substrates.

ACKNOWLEDGEMENT

Financial support by the National Research Foundation and The World Academy of Science is gratefully acknowledged.

REFERENCES

[1] A. H. Rashed, "Properties and Characteristics of Silicon Carbide," POCO Graphite, Inc, vol. 5, no. 7, 2002.

[2] R. Devanathan, W. J. Weber, and F. Gao, "Atomic scale simulation of defect production in irradiated 3C-SiC," *J. Appl. Phys.*, vol. 90, no. 5, pp. 2303–2309, 2001.

[3] T. T. Hlatshwayo, N. G. Van Der Berg, M. Msimanga, J. B. Malherbe, and R. J. Kuhudzai, "Iodine assisted retainment of implanted silver in 6H-SiC at high temperatures," *Nucl. Instruments Methods Phys. Res. Sect. B Beam Interact. with Mater. Atoms*, vol. 334, pp. 101–105, 2014.

[4] J. B. Malherbe, “Diffusion of fission products and radiation damage in SiC,” *J. Phys. D. Appl. Phys.*, vol. 46, no. 47, pp. 1–52, 2013.

[5] M. Feltus, F. Poc, P. Winston, and T. Poc, “Fission Product Transport in TRISO Particle Layers Under Operating and Off-Normal Conditions,” no. 10.

[6] J. Peterson, M. MacDonell, L. Haroun, and F. Monette, “Selenium,” *Radiol. Chem. Fact Sheets to Support Heal. Risk Anal. Contam. Areas*, no. October, pp. 46–47, 2007.

[7] American Elements, accessed March 09, 2019, Selenium *www.americanelements.com.*

[8] Y. Katoh, L. L. Snead, I. Szlufarska, and W. J. Weber, “Radiation effects in SiC for nuclear structural applications,” *Curr. Opin. Solid State Mater. Sci.*, vol. 16, no. 3, pp. 143–152, 2012.

[9] E. Friedland, T. Hlatshwayo, and N. van der Berg, “Influence of radiation damage on diffusion of fission products in silicon carbide,” *Phys. Status Solidi*, vol. 10, no. 2, pp. 208–215, 2013.

[10] R. Devanathan, W. J. Weber, and F. Gao, “Atomic scale simulation of defect production in irradiated 3C-SiC,” *J. Appl. Phys., vol. 90, no. 5, pp. 2303–2309, 2001*.

[11] J. B. Malherbe, P. A. Selyshchev, O. S. Odutemowo, C. C. Theron, E. G. Njoroge, D. F. Langa and T. T. Hlatshwayo, “Diffusion of a mono-energetic implanted species with a Gaussian profile,” *Nucl. Instruments Methods Phys. Res. Sect. B Beam Interact. with Mater. Atoms*, vol. 406, pp. 708–713, Sep. 2017.

[12] J. F. Ziegler, “SRIM 2012 computer code-2012,” www.srim.org, accessed Nov. 16, 2018.

[13] T. T. Hlatshwayo, L. D. Sebitla, E. G. Njoroge, M. Mlambo, and J. B. Malherbe, “Annealing effects on the migration of ion-implanted cadmium in glassy carbon,” *Nucl. Instruments Methods Phys. Res. Sect. B Beam Interact. with Mater. Atoms*, vol. 395, pp. 34–38, 2017.

[14] F. Gao and W. J. Weber, “Cascade overlap and amorphization in 3C-SiC: Defect accumulation, topological features, and disordering,” *Phys. Rev. B - Condens. Matter Mater. Phys.*, vol. 66, no. 2, pp. 1–10, 2002.

[15] J. B. Malherbe, N. G. Van Der Berg, R. J. Kuhudzai, T. T. Hlatshwayo, I. Festkörperphysik, and F. Jena, “Scanning Electron Microscopy of the Surfaces of Ion Implanted SiC,” *Nucl. Inst. Methods Phys. Res. B*, vol. 354, pp. 23–27, 2015.

[16] A. Deslandes, M. C. Guenette, L. Thomsen, M. Ionescu, I. Karatchevtseva, and G. R. Lumpkin, “Retention and damage in 3C- b SiC irradiated with He and H ions,” *J. Nucl. Mater.*, vol. 469, pp. 187–193, 2016.

[17] S. Nakashima and H. Harima, “Raman Investigation of SiC Polytypes,” *phys. stat. sol.*, vol. 162, pp. 39–64, 1997.

[18] D. W. Feldman, J. H. Parker, W. J. Choyke and L. Patrick, **“**Phonon dispersion curves by raman scattering in SiC, Polytypes 3 C, 4 H, 6 H, 15 R, and 21 R**,”** *Physical Review,* vol. 173(3), pp 787, 1968.

[19] W. Chang, Z. C. Feng, J. Lin, R. Liu, A. T. S. Wee, K. Tone, and J. H. Zhao. "Infrared reflection investigation of ion-implanted and post-implantationannealed epitaxially grown 6H-SiC," *Surf.Interface Anal.* 33, no. 6, pp. 500-505, 2002.

[20] G. Litrico, N. Piluso, and F. La Via. "Detection of crystallographic defects in 3C-SiC by micro-Raman and micro-PL analysis," *InMaterials Science Forum, Trans Tech Publications,* Vol. 897, pp. 303-306, 2017.

[21] E. Wendler, T. Bierschenk, F Felgenträger, J.Sommerfeld, W. Wesch, D. Alber, G. Bukalis, L. C. Prinsloo, N. Van der Berg, E. Friedland and J. B. and Malherbe, “Damage formation and optical absorption in neutron irradiated SiC,” *Nucl. Inst. Methods Phys. Res. B*, vol. 286, pp. 97–101, 2012.

[22] X. Feng, Y. Zang. "Raman scattering properties of structural defects in SiC," *In 2016 3rd International Conference on Mechatronics and Information Technology. Atlantis Press.*